THE ASTROPHYSICAL JOURNAL, 263:325–339, 1982 December 1

SIMULTANEOUS OPTICAL AND X-RAY BURSTS FROM 4U/MXB 1636−53

H. PEDERSEN AND J. LUB
European Southern Observatory
H. INOUE, K. KOYAMA, K. MAKISHIMA, M. MATSUOKA, K. MITSUDA, T. MURAKAMI, M. ODA, Y. OGAWARA, T. OHASHI, N. SHIBAZAKI, AND Y. TANAKA
Institute of Space and Astronautical Science
S. HAYAKAWA, H. KUNIEDA, F. MAKINO, K. MASAI, F. NAGASE, AND Y. TAWARA
Department of Astrophysics, Faculty of Science, Nagoya University
S. MIYAMOTO, H. TSUNEMI, AND K. YAMASHITA
Department of Physics, Faculty of Science, Osaka University
I. KONDO
Institute for Cosmic Ray Research, University of Tokyo
AND
J. G. JERNIGAN, J. VAN PARADIJS,[1] A. BEARDSLEY, L. COMINSKY, J. DOTY, AND W. H. G. LEWIN
Department of Physics and Center for Space Research, Massachusetts Institute of Technology
Received 1981 August 31; accepted 1982 May 19

ABSTRACT

We report the detection of five coincident optical/X-ray bursts from 4U/MXB 1636−53. The optical observations were made with the Danish 1.5 m telescope at the European Southern Observatory (E.S.O.) and the X-ray observations were made with the *Hakucho* X-ray observatory. This is the first time that more than one coincident burst has been observed from a single source. We have analyzed these bursts in terms of a simple general mathematical model, in which the optical emission (both during and between the bursts) is that of a blackbody and the result of thermally reprocessed X-rays. One expects that the optical burst is a delayed and smeared version of the X-ray burst. We estimate that the optical radiative delay is smaller than the observed values, which we believe are therefore mainly due to the geometry of the system. For the delay and smearing of the optical burst and the maximum temperature of the reprocessing region, we find values of ~ 2.5 s, < 4 s, and $\sim 75 \times 10^3$ K, respectively. The reprocessing region surrounding the X-ray source has a projected area of $\sim 6 \times 10^{21}$ cm^2 corresponding to a linear size of ~ 1.5 lt-sec independent of any assumption about its geometry. An accretion disk around a compact object is one plausible model for the reprocessing region. The derived restrictions on the parameters of the reprocessing region also constrain the parameters of a consistent low-mass close binary system containing an $\sim 1.4\ M_\odot$ neutron star. The radius of the accretion disk is > 1.5 lt-sec, the mass of the Roche lobe filling companion star is $< 2.0\ M_\odot$ corresponding to a binary period between ~ 1 hour and ~ 10 hours.

Subject headings: stars: individual — X-rays: binaries — X-rays: bursts

I. INTRODUCTION

The object 4U/MXB 1636−53 is a member of the class of "galactic bulge sources" with the following characteristics (for recent reviews see Lewin and Clark 1980; Lewin and Joss 1981, 1982, and references therein): (1) Its starlike optical counterpart is faint in contrast to the luminous massive X-ray binary systems; (2) Its optical spectrum is devoid of normal stellar absorption features; (3) The apparent ratio of X-ray to optical luminosity is $\sim 10^3$. For the massive systems this ratio is several orders of magnitude lower. As is the case for many galactic bulge sources, 4U/MXB 1636−53 is a type I X-ray burst source. In contrast, no type I X-ray bursts have been observed from any of the massive binary X-ray systems. A type I burst (Hoffman, Marshall, and Lewin 1978) is believed to be the result of a thermonuclear flash on the surface of a neutron star (for reviews see, e.g., Lewin and Joss 1981, 1982).

Extensive optical and simultaneous optical and X-ray observations have been made of several of the brightest galactic bulge sources for which an optical counterpart is known (for reviews see Lewin and Joss 1981, 1982, and references therein). Among them are several close binary systems with low-mass ($\lesssim 1\ M_\odot$) companion stars (Oke 1977; Thorstensen, Charles, and Bowyer 1978; van Paradijs *et al.* 1980; Middleditch *et al.* 1981), and it is generally believed that galactic bulge sources, as a

[1] Astronomical Institute, University of Amsterdam, The Netherlands.

class, are low-mass close binary systems. The optical emission is largely the result of X-ray heating of the accretion disk (McClintock *et al.* 1979; McClintock *et al.* 1980; Canizares *et al.* 1980). Simultaneous optical and X-ray observations of two type I X-ray burst sources have shown that the optical bursts trail the X-ray bursts by a few seconds (McClintock *et al.* 1979; Hackwell *et al.* 1979), and it has been suggested that this delay is due to travel time differences.

In this paper we discuss how one can obtain information about the geometry of X-ray burster systems from simultaneous optical and X-ray observations, and we report on such simultaneous observations of 4U/MXB 1636−53. The type I X-ray bursts serve as a probe; they illuminate the surroundings of the compact object which subsequently reveal their presence by optical radiation. By comparing the changes in the observed X-ray fluxes (probing signal) with the responding optical fluxes from the surroundings, one can deduce information about these surroundings.

In § II we describe the simultaneous X-ray and optical observations of 4U/MXB 1636−53. In § III we discuss the physical idea of an optical burst being due to reprocessing of an X-ray burst in material in the vicinity of the compact object. This results in a modification of the X-ray burst signal, which we describe in terms of an optical response function (delay, smearing). Delay and smearing due to radiative processes are discussed in § III*a*; those due to the geometry are discussed in § III*b*. In § IV we discuss the method of analysis; in § V we give the results which we follow by a discussion in § VI.

In the companion paper the optical bursts from 4U/MXB 1636−53 are discussed (Pedersen *et al.* 1982).

II. OBSERVATIONS

a) Optical Observations

As part of the 1979 world-wide coordinated burst watch (Lewin 1979) a total of 46 hours of high speed photometry of 4U/MXB 1636−53 was done during the periods 1979 June 20–July 2 and July 20–August 3 using the Danish 1.5 m telescope at La Silla. A total of 15 optical bursts were detected (Pedersen *et al.* 1979; Pedersen *et al.* 1982), five of these in coincidence with X-ray bursts (see Fig. 2). The first five rows of Table 1 describe the sky condition and the instrumentation which was used on the nights when the five coincident bursts were detected. Most of the time, the seeing was good so that small ($\lesssim 10\farcs5$) entrance diaphragms could be used; this was of importance in view of the faintness of the object ($m_v = 17.5$; McClintock *et al.* 1979). However, some nights were affected by cirrus, and the resulting photometry is therefore less accurate.

The photometer is a one-channel instrument used with pulse counting electronics. The only two optical elements between the telescope and the Peltier-cooled photomultiplier are an ultraviolet transmitting Barlow lens, which changes the beam from f/8.6 to f/15, and a Fabry lens, which also serves as an entrance window to the cold box. Both lenses are made from antireflection glasses. Guiding was done using the main field mirror together with the integrating TV system. The guiding was checked about five times per hour, thereby interrupting measurements. Corrections to the telescope's position were usually 1″ or less. Both the counts and timing information were recorded on magnetic tape. The last few minutes of data were also displayed on an oscilloscope screen which was constantly monitored for the presence of bursts. The sixth and seventh row of Table 1 summarize the timing information for the five coincident bursts. Although the length of individual data integrations and dead time between the integrations varied, the timing was kept accurate to 20 ms by oscilloscopic comparison of the computer clock strobe with the 15 MHz WWV radio signals. A correction for the delay of WWV relative to UT was applied during the data reduction.

The diaphragm was kept centered on a position ∼1″ south of the burst source (McClintock *et al.* 1977) in order to avoid a possible contribution from a brighter star ∼7″ to the north. Sky measurements were taken at a position ∼12″ east, ∼1″ north of the burster and are given in the last row of Table 1.

Taking account of the transmission functions of all the optical components of the photometer (from the atmosphere to the photomultiplier) we arrive at an

TABLE 1

OPTICAL INSTRUMENTAL INFORMATION AND CONDITIONS

	JUNE 21			JUNE 28	JULY 28
PARAMETER	0017 (UT)	0148 (UT)	0334 (UT)	0155 (UT)	0115 (UT)
Sky condition	Light cirrus	Light cirrus	Light cirrus	Photometric	Cirrus
Fabry lens	Glass	Glass	Glass	Glass	Spectrosil
Filter	10 mm $CuSO_4$	10 mm $CuSO_4$	10 mm $CuSO_4$	None	None
Diaphragm	10″.5	10″.5	10″.5	10″.5	7″
Photomultiplier	EMI 9659 QA	EMI 9659 QA	EMI 9659 QA	EMI 9789 QB	EMI 9789 QB
Integration time	300 ms	300 ms	300 ms	200 ms	200 ms
Dead time between integrations	88 ms	93 ms	90 ms	77.0 ms	32.3 ms
Sky (counts s^{-1})	346	347	344	308 ± 6	...

equivalent photometric bandpass of ~1870 Å and an effective wavelength of

$$\lambda_{\rm eff} = \int_0^\infty \lambda S_\lambda d\lambda \Big/ \int_0^\infty S_\lambda d\lambda \approx 4300 \text{ Å}, \quad (1)$$

where S_λ is the transmission function.

The absolute energy calibration of the photometer was obtained by observing the absolutely calibrated white dwarf standard star Wolf 485A (Oke 1974). On several nights we also observed the Sd 0 star Feige 110 (Stone 1977). From a comparison between W485A and Feige 110 it appears that the effect of the extremely blue continuum of the latter ($U-B=-1.2$) causes only a $\sim 6\% \pm 3\%$ difference in the conversion of flux to counts with reference to W485A ($U-B=-0.6$). $(U-B)$ is the relevant color since our bandpass encompasses mainly the U and B regions. Since the colors of the quiescent burster ($U-B=-0.7$; McClintock *et al.* 1977) and the calibration stars are rather similar, it is therefore not necessary to apply a color correction when converting the observed count rates of the burster to energy flux. The bursts are assumed to have the same color as the object in its quiescent state.

The first three rows of Table 2 give the count rates and equivalent fluxes determined from the observations of these standard stars for the optical "persistent source" as well as the peaks of the five coincident bursts and their total integrated fluxes. The quoted errors are a combination of statistical uncertainties and estimated systematical errors in the energy calibration. However, light cirrus was present during the nights June 20/21 and July 27/28, which may have introduced nonstatistical errors which may be of the order 10%–20%.

b) *X-Ray Observations*

The X-ray observations of 4U/MXB 1636−53 were performed with the burst monitor system on the *Hakucho* X-Ray Observatory (Kondo *et al.* 1981). This system consists of three rotating modulation collimators (RMC) as well as one tubular collimator, with fields of view along the direction of the satellite spin axis. The RMC systems have two coarse modulation collimators (CMC 1 and 2) with circular (17°.4 FWHM) fields of view. The two RMC systems have a band spacing of 283′, but they are out of phase by 180°, so that the sum of the two produces a nonmodulated signal. The CMC system

TABLE 2

SUMMARY OF THE OPTICAL AND X-RAY OBSERVATIONS IN 1979

PARAMETER	JUNE 21			JUNE 28	JULY 28
	0017 (UT)	0148 (UT)	0334 (UT)	0155 (UT)	0115 (UT)
Optical "Persistent Source" (rate above sky background)[a]:					
Counts s^{-1}	138 ± 8	121 ± 6	>74[b]	157 ± 8	>109[c]
Ergs cm^{-2} s^{-1}	$(5.5 \pm 0.5) \times 10^{-13}$	$(4.8 \pm 0.5) \times 10^{-13}$	$>0.3 \times 10^{-12}$ [b]	$(5.0 \pm 0.6) \times 10^{-13}$	$>4.3 \times 10^{-13}$
Optical Burst Peak (Maximum Rate above "Persistent Source")[a]:					
Counts s^{-1}	Not observed	122 ± 20	...	325 ± 16	>148
Ergs cm^{-2} s^{-1}	...	$(4.8 \pm 0.8) \times 10^{-13}$	...	$(1.0 \pm 0.15) \times 10^{-12}$	$>0.5 \times 10^{-13}$
Optical Integrated Burst Energy[a]:					
Counts	...	1364 ± 200	>1750	5711 ± 360	>2353
Ergs cm^{-2}	...	$(5.5 \pm 0.8) \times 10^{-12}$	$>6.8 \times 10^{-12}$	$(1.8 \pm 0.2) \times 10^{-11}$	$>0.75 \times 10^{-11}$
X-ray "Persistent Source" (rate above X-ray and particle background)					
Ergs cm^{-2} s^{-1}	$(1.0 \pm 0.3) \times 10^{-9}$	$(1.0 \pm 0.3) \times 10^{-9}$	$(1.0 \pm 0.3) \times 10^{-9}$	$(1.1 \pm 0.2) \times 10^{-9}$	$\sim 1.0 \times 10^{-9}$ [e]
Bolometric X-ray Burst Peak[d] (Maximum Rate above the "Persistent Source")					
Ergs cm^{-2} s^{-1}	$(5.7 \pm 0.7) \times 10^{-8}$	$(1.0 \pm 0.4) \times 10^{-8}$	$(1.5 \pm 0.4) \times 10^{-8}$	$(3.4 \pm 0.3) \times 10^{-8}$	$(1.9 \pm 0.7) \times 10^{-8}$ [e]
X-ray Integrated Bolometric[d] Burst Energy					
Ergs cm^{-2}	$(2.80 \pm 0.3) \times 10^{-7}$	$(1.2 \pm 0.6) \times 10^{-7}$	$(1.6 \pm 0.3) \times 10^{-7}$	$(3.4 \pm 0.1) \times 10^{-7}$	$(1.9 \pm 0.4) \times 10^{-7}$ [e]
Optical/X-ray Integrated burst fluxes	...	$(4.6 \pm 2.4) \times 10^{-5}$ $[(6.0 \pm 3.1) \times 10^{-4}]$[f]	$>4.3 \times 10^{-5}$ $[>5.6 \times 10^{-4}]$[f]	$(5.3 \pm 0.6) \times 10^{-5}$ $[(6.9 \pm 0.8) \times 10^{-4}]$[f]	$>3.9 \times 10^{-5}$ [e] $[>5.1 \times 10^{-4}]$[e,f]

[a] Integrated over 3350–5250 Å; not corrected for extinction; see § IV.

[b] Due to poor centering of the star in the diaphragm, these values may be low by a factor of at most 2.

[c] Cirrus.

[d] Bolometric; indicates that the total flux is calculated assuming a Planck spectrum.

[e] Calculations based on CMC (17°.4 FWHM) data.

[f] The values between square brackets have been corrected for interstellar absorption. The uncertainty in this correction is about a factor of 2 (see § IV).

can determine source locations to an accuracy of ~0°.5. A fine modulation collimator (FMC 1) may be used to locate positions to within a few arc minutes. The tubular detector (FMC 2) is not equipped with a modulation collimator and thus provides a nonmodulated signal for comparison. Both FMC 1 and 2 have circular (5°.8 FWHM) fields of view. Further details describing the *Hakucho* spacecraft are given elsewhere (Kondo *et al.* 1981).

The X-ray observations of 4U/MXB 1636−53 were carried out during two time intervals: 1979 June 20–July 2 and July 26–August 2. Coincident optical/X-ray bursts were detected on five occasions (Pedersen *et al.* 1979). The bursts which occurred on 1979 June 21 and June 28 were detected by both the FMC and CMC systems. The burst which occurred on July 28 was detected by the CMC 1 and 2 system only, as 4U/MXB 1636−53 was outside the field of view of the FMC systems. All five bursts were associated with 4U/MXB 1636−53 (the two combined CMC systems yield a positional accuracy ~0°.5).

c) Coincident Optical and X-Ray Bursts

In Figure 1 the time intervals of X-ray and optical observations are indicated, together with the bursts detected in these intervals. The X-ray observing intervals include gaps due to Earth occultation of the X-ray source, and high particle background (in the South Atlantic Anomaly). These gaps are only indicated when an optical burst occurred within them (indicated by "O"). Similarly, the optical coverage contains gaps for sky calibration, guiding control, etc., which are not shown.

Figure 2 shows the five coincident optical bursts, the FMC 2 detections of the first four bursts in two energy channels, as well as the sum of the CMC signals for all five coincident optical/X-ray bursts. Shortly before the first event, the star was not centered in the telescope diaphragm, and while this was being corrected using the TV system, the burst was observed to occur. Since the TV system used a centerfield mirror, the data acquisition system measured only dark current during most of this optical burst. The subsequent rise in the count rate (in this case only) is due to the mirror moving out of the beam, and is not the actual rise of the burst. The decaying portion of this first burst is real, however. This burst and the next two bursts all occurred during the night of June 21, separated by ~1.5 hours. These three bursts are all type I X-ray bursts (Hoffman, Marshall, and Lewin 1978).

Coincident burst four, which was detected one week later on 1979 June 28 is a large one. The rise time of the burst is approximately 5 s in both the X-ray and optical data, and the integrated energy in this burst is greater than in any one of the other four coincident bursts (see Table 2).

In Table 2 we summarize for five bursts some observational results and reduced values for the persistent fluxes and the peak burst fluxes (optical and X-ray) and the integrated bolometric burst energy (see § IV). The ratios of optical to X-ray integrated burst fluxes are shown at the bottom of Table 2.

Optical bursts were observed on 1979 July 29, UT 0128 and on July 29, UT 2329. There is some doubt about these optical bursts, since the Moon was up. The *Hakucho* observatory observed the source at these times and did not detect any significant X-ray increase. Two sigma upper limits of the X-ray peak bursts fluxes and the integrated (over 30 s) fluxes were 8.0×10^{-11} ergs cm^{-2} s^{-1} and 4.4×10^{-10} ergs cm^{-2}, respectively, on July 29, UT 0128 and they were 6.2×10^{-11} ergs cm^{-2} s^{-1} and 3.4×10^{-10} ergs cm^{-2}, respectively, on July 29, UT 2329. Because the optical bursts are in

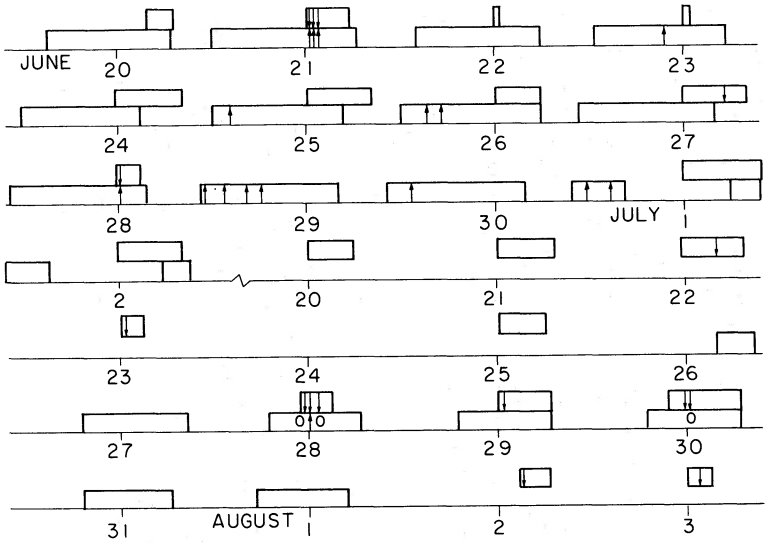

FIG. 1.—1979 E.S.O./*Hakucho* observing periods of 4U/MXB 1636−53 in the optical (*upper traces*) and the X-ray (*lower traces*) portion of the spectrum. Bursts are indicated with arrows. The arrows representing optical bursts are pointing down, and those indicating X-rays bursts are pointing up. The Os indicate detections of optical bursts at times that the X-ray source was occulted by the Earth.

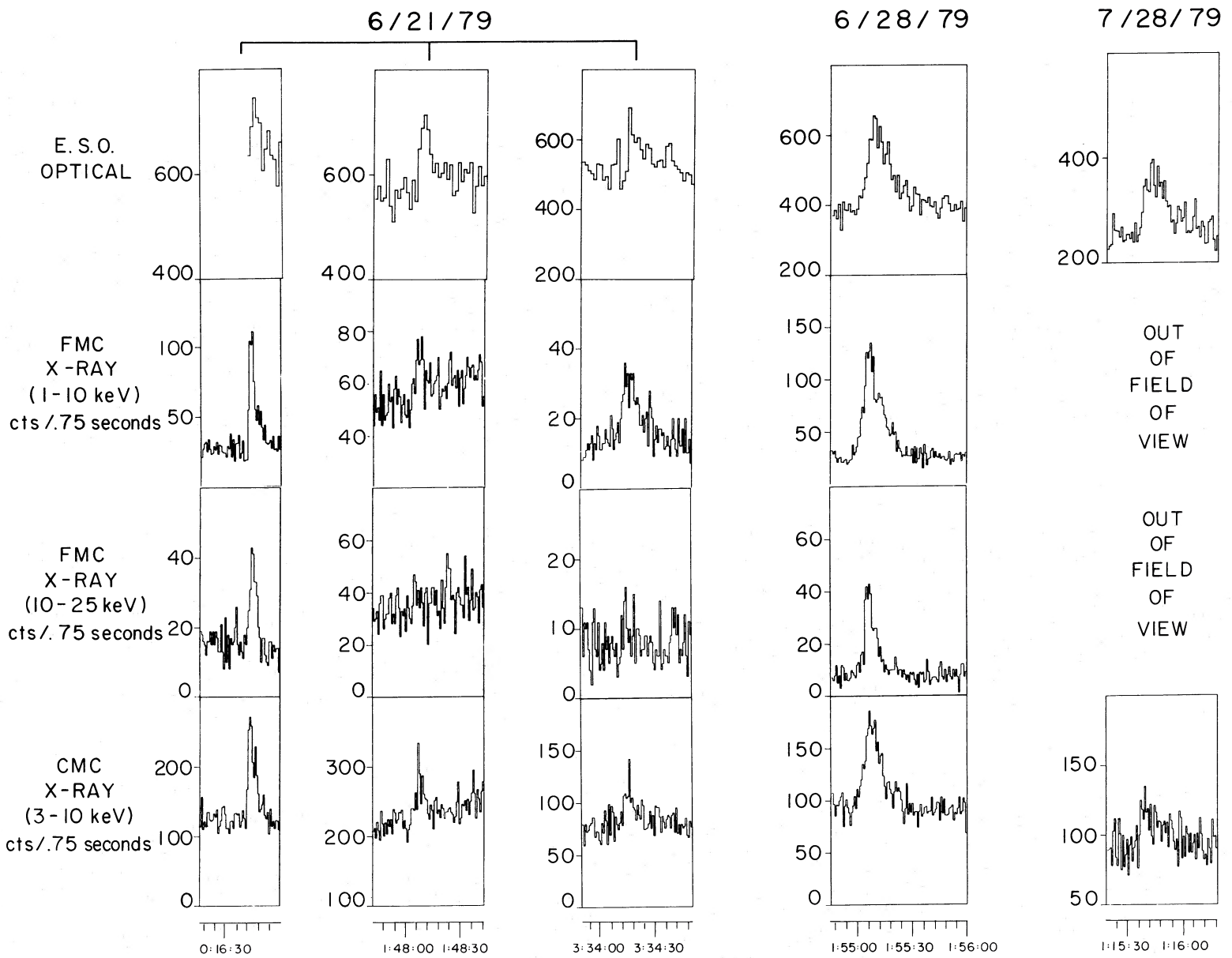

FIG. 2.—E.S.O./*Hakucho* observations of MXB 1636−53: simultaneous optical and X-ray data for five bursts

question, these bursts are not further discussed, and they are not listed in Table 2. It seems possible, however, that these optical bursts were real bursts in which case the absence of detection of X-ray bursts is very interesting. This warrants further investigation.

III. THEORETICAL CONSIDERATIONS ON SIMULTANEOUS OPTICAL AND X-RAY BURSTS

In previous coincident optical and X-ray bursts, observed from 4U/MXB 1735−44 and MXB 1837+05 (=Ser X-1 = 4U 1837+04) the optical bursts were observed a few seconds after the X-ray bursts (McClintock *et al.* 1979; Hackwell *et al.* 1979), and the ratio of the integrated flux in the optical burst (corrected by us, for interstellar extinction; see Neckel and Klare 1980; Hammerschlag-Hensberge, McClintock, and van Paradijs 1981; Thorstensen, Charles, and Bowyer 1980) to that in the X-ray burst was of the order of 10^{-4}. This value is too large by about six orders of magnitude to explain the optical emission as the extrapolation of the blackbody X-ray burst spectrum toward longer wavelengths (Swank *et al.* 1977; Hoffman, Lewin, and Doty 1977*a*, *b*). The observed energy ratio and the measured delay of the optical bursts indicate that they are the result of reprocessing of X-rays near the X-ray burst source. Matter in the vicinity of the burst source absorbs part of the X-rays, gets heated, and reradiates the absorbed energy with a frequency distribution related to its temperature.

The delay and smearing of the optical burst is the result of radiative processes and the geometry of the system.

a) Radiative Transport Delay and Radiative Smearing

We have considered the effect of radiative transport on the time smearing following work by L. Petro (1981, private communication). The absorption of X-rays and the subsequent emission of optical photons do not occur instantaneously and at the same time. There is a radiative delay and radiative smearing of the optical flux relative to the X-ray flux. The X-rays, mainly in the range between 1 and 20 keV, penetrate a gaseous absorber and, possibly after many scatterings, are absorbed. The energy deposited in the absorber must diffuse out via radiative transfer of photons whose characteristic energy is of the order of a few eV. The energy escaping as optical photons can be described by a diffusion function, which delays and smears out the original incoming X-ray signal. Detailed calculations of the diffusion of photons from an atmosphere show that to within a factor of order unity the smearing of the signal equals the average delay (Chandrasekhar 1943; Sunyaev and Titarchuk 1980).

In the Appendix we have calculated an estimate of the effect of radiative reprocessing, extending the earlier work of Chester (1978, 1979). Our results are in reasonable agreement with those of Chester for X-ray photons below 8 keV but are not in agreement for photons with energies larger than 8 keV; our estimate yields a faster response time scale of order of ~ 1 s for X-ray energies <15 keV. However, both results (Chester's and ours) do not incorporate the following complications:

1. The total X-ray energy deposited significantly alters the state (e.g., temperature, size, shape, density) of the reprocessor.
2. The albedo of the reprocessor is strongly energy dependent. Therefore, a small fraction of the energy in hard X-rays is deposited, possibly resulting in a shorter reprocessing time scale.
3. The radiative reprocessing time scale includes not only the random walk travel time as calculated by Chester (1978, 1979) and in the Appendix, but also includes a finite interaction time for each step of the random walk (R. London, private communication). Since the effect is strongly dependent on the density at the site of the X-ray energy deposit, it could possibly result in a long reprocessing time scale even for soft X-rays.

b) Geometric Delay and Geometric Smearing

The combined pathlength of the absorbed X-rays and the subsequently emitted optical photons toward the observer is longer than that of the X-rays which are emitted directly toward the observer. This will cause a delay of the optical signal. Since the reprocessing body is of finite extent, different parts of it will give rise to different values of this geometric delay and consequently a geometric smearing of the optical signal.

The optical response of a reprocessing object to infalling X-rays provides a probe of the structure of the material in the near vicinity of the X-ray source. An X-ray burst is a particularly good probe of the spatial geometry of the circumsource material because of the large and rapid excursion of X-ray luminosity. Since the radiative delay and smearing are small (see § III*a*), we will assume the optical response is completely determined by the spatial parameters of a finite reprocessing object.

The basic principles of our model are similar to those used in the synthesis of optical light curves of massive X-ray binaries (see, e.g., Wickramasinghe and Whelan 1975; Zuiderwijk *et al.* 1977). The surface of the reprocessing object is modeled as a collection of many differential surface elements. At each of these elements a fraction $f = (1 - \text{albedo})$ of the infalling X-rays is absorbed. Our basic assumption is that all absorbed X-ray energy is reemitted in the form of blackbody radiation. Detailed calculations of the optical spectrum emitted by an X-ray heated stellar atmosphere (see, e.g., Milgrom and Salpeter 1975; London, McCray, and Auer 1980) indicate that the deviations from a Planck curve are small, and that $f = 0.5$ is a typical value.

Since we assume that a fraction f of the intercepted X-ray energy is reemitted, the surface element obtains an effective temperature T_e (for a given value L_x of the X-ray luminosity) according to

$$\sigma T_e^4 = f L_x \frac{\cos \gamma}{4\pi r^2} + \sigma T_q^4 . \qquad (2)$$

Here r is the distance from the surface element of the absorber to the X-ray source; γ is the angle between

the surface normal and the direction of the infalling X-rays; T_q is the effective temperature of the surface element in the absence of X-ray heating; and σ is the Stefan-Boltzmann constant. The additional heat input implied by the term σT_q^4 is provided by internal energy of the reprocessing material. The flux at frequency ν measured by an observer at distance d is

$$F_\nu = \frac{1}{d^2}\int_{\text{surface}} B_\nu(T_e)\cos\xi dA \tag{3}$$

(it is assumed here that limb-darkening [or brightening] plays no role). Here, B_ν is the Planck function, and ξ is the angle between the normal to the surface and the direction toward the observer. For any real geometries the integral of equation (3) must exclude those surface elements which are shadowed from the X-rays or whose reprocessed radiation is shadowed as viewed by a distant observer.

Since all flux measurements are resolved temporally but not spatially, approximate estimates of the physical properties of the reprocessing region require spatial averaging. The simplest possible model is to assume a single plate of area A separated from the X-ray source by distance r. The angles γ and ξ are assumed to be constant. In this approximation, the temporal profile of the optical emission at frequency ν measured at the Earth is

$$F_\nu(t) = \frac{A_{\text{eff}}}{d^2} B_\nu(T_e)\,, \quad A_{\text{eff}} = A\cos\xi\,, \tag{4a}$$

where

$$T_e(t) = \left[\frac{L_x(t-\Delta)+H}{L_{\max}+H}\right]^{1/4} \times T_{\max}\,, \tag{4b}$$

and

$$H = \frac{4\pi r^2 \sigma T_q^4}{f\cos\gamma}\,. \tag{4c}$$

The total flux from the reprocessing object measured at distance d is calculated by integrating over the entire visible surface of the reprocessing object. The parameters $L_{\max}$ and $T_{\max}$ are the maximum values of the X-ray luminosity and the maximum temperature of the reprocessing object, respectively. Incorporating all the spatial parameters into these two quantities crudely approximates the exact integral given by equation (3). The dependence of the flux F_ν on the parameter γ is incorporated into the selection of the parameter $T_{\max}$. The time dependence of the flux F_ν is determined by the X-ray luminosity L_x which occurred at an earlier time defined by the difference in light travel time, Δ, between the reprocessed radiation and direct X-rays. Equation (4) models the gross properties of the temporal profile of the reprocessed radiation. In a real system the elements of a finite reprocessing region would have a range of differences in light travel time. The definition of $T_e(t)$ may be generalized by replacing $L_x(t-\Delta)$ with a convolution of $L_x(t)$ with a light travel distribution function $g(t)$ which models the geometry of the system.

$$L_x(t-\Delta) \rightarrow \int_{-\infty}^{\infty} L_x(\tau)g(t-\tau)d\tau\,. \tag{5}$$

The distribution function $g(t)$ is nonzero only for positive value of time t (this ensures causality), and its integral is normalized to unity. The simple case of a fixed delay Δ would correspond to setting $g(t) = \delta(t-\Delta)$. In general delay corresponds to the time of the peak of $g(t)$ and smearing corresponds to the width of $g(t)$. Together, equations (4) and (5) provide an approximate model of any reprocessing object in which the bulk of the radiation is produced by a region with a distribution of temperatures peaked around a single value. This is often true even for complex geometries since some portion of the object will emit most of the radiation due to its favorable value of γ or ξ. Note that the spectrum of the radiation is assumed to be that of a blackbody at each instance of time, even though smoothing implies a blend of temperatures.

IV. METHOD OF ANALYSIS

We assume that the X-ray flux (both the persistent component and the burst component) is isotropically emitted from a region, at or close to the surface of a neutron star. Therefore the observed X-ray flux is a direct measure of the energy input into the reprocessing object.

Our analysis method requires that the measured broad-band X-ray flux represents approximately the total energy flux emitted by the X-ray source. This assumption precludes any significant ultraviolet, soft X-ray (<1 keV), or hard X-ray (>25 keV) radiation. Also the effects of obscuration of X-rays by circumsource material or the interstellar medium are assumed to be negligible.

a) Measured X-Ray Flux—Bolometric X-ray Flux

The X-ray flux is measured in two broad energy channels. A linear combination of the X-ray count rates in these two channels approximates the total bolometric X-ray flux, F_x, (within 5%) under the assumption that the spectrum is that of a blackbody with a temperature between 1.5 and 3.0 keV.

$$F_x\Delta_x = K_A(A - N_A) + K_B(B - N_B) \tag{6}$$

Table 3 contains the numerical values of all constants in this section. A and B are the total counts detected in each X-ray channel for integration times of Δ_x (=0.1875 s). N_A and N_B are estimates of the nonsource component of the count rates. The calculations of the coefficients K_A and K_B include the implied flux outside the energy boundaries of the detector and incorporate the variation in sensitivity as a function of energy. Since the channels have broad-band response and the flux peaks in X-rays, this simple expression for the total energy flux assuming a blackbody of X-ray temperature even approximates the flux if the deviations from a

TABLE 3

BURST ON 1979 JUNE 28, 0155 UT

Defined Parameter	Symbol	Value
X-ray time resolution	Δ_x	0.1875 s
X-ray bolometric constants	K_A	1.0×10^{-10} ergs cm^{-2} s^{-1}
	K_B	3.7×10^{-10} ergs cm^{-2} s^{-1}
Optical bolometric constant	K_o	$(4.3 \pm 0.7) \times 10^{-15}$ ergs cm^{-2} s^{-1}
Optical time resolution	Δ_o	0.2768 s
Optical passband temperature	T_{ph}	33×10^3 K ($kT_{ph} = 2.9$ eV)
Optical passband width	$\Delta\nu$	3.0×10^{14} Hz (1870 Å)
Optical passband	ν	7.0×10^{14} Hz (4300 Å)
Extinction factor (4300 Å)	K_e	~4–20 (2.8 mag)

blackbody spectrum are substantial. There is much support for the assumption of the approximate blackbody spectrum for X-ray bursts (Swank *et al.* 1977; Hoffman, Lewin, and Doty 1977*a*, *b*); however, the methodology here only requires that some fraction of the total X-ray energy is reprocessed independent of its spectrum.

b) Response of the Reprocessor

The reprocessed radiation is a superposition of contributions from different parts of the reprocessing body, each having its own temperature. In the case of a variable X-ray luminosity (during bursts) the optical signal at a given time results from the X-ray signal at various earlier times. Following the formulation given in § III, we assume a spatially averaged relation between the X-ray flux and the reprocessed radiation. In particular the spectrum of the reprocessed radiation is assumed to be precisely blackbody at each instance. The spatial extent of the reprocessing object predominantly results in a temporal spreading of the reprocessed radiation compared to the incident X-radiation. The primary effects are the delay and smearing of the optical signal relative to the X-ray signal. The temperature blending due to the spatial extent is ignored.

The optical photometry passband (3350–5250 Å) corresponds to an average photon energy $kT_{ph} \approx 2.9$ eV, whence $T_{ph} \approx 33 \times 10^3$ K. Since the passband only accepts a small fraction of the reprocessed radiation and photometry is available in only a single color, the total energy reradiated cannot be directly calculated.

The energy radiated within the frequency passband $\Delta\nu$ (see Table 3) is

$$F_o \Delta_o = K_e K_o (O - N_o) . \quad (7)$$

O is the total counts detected in each integration bin of duration Δ_o. N_o is an estimate of the nonsource component of the count rate. The value of K_o was determined from measurements of standard stars and includes an air mass correction. The coefficient K_e is a correction factor for the effect of absorption by the interstellar medium. The value for K_e has been estimated from the reddening distance relation in the direction of 4U/MXB 1636−53, and independently from an assumption about the intrinsic color indices of the source.

c) Interstellar Absorption

According to Lucke (1978) the interstellar reddening in the direction of 4U/MXB 1636−53 $(B-V) = 0.4$ mag kpc^{-1}. Since the length through the interstellar dust layer (assumed to have a thickness of 150 pc; see Allen 1973) in this direction equals ~1800 pc, the total reddening $E(B-V) \sim 0.7$ mag, and the extinction of the optical flux (passband centered on 4300 Å) equals ~2.8 mag, thus the extinction $K_e \approx 13$. Using the recent computation of reddening data by Neckel and Klare (1980), we find that $E_{B-V} = 0.4$ out to a distance of ~5 kpc, corresponding to $K_e \approx 4.4$.

If we assume that the intrinsic colors of 4U/MXB 1636−53 are the same as those of Sco X-1 and 4U/MXB 1735−44 (see Hammerschlag-Hensberge *et al.* 1981; van Paradijs 1981) we get

$$E_{B-V}(\text{4U/MXB 1636}-53) = E_{B-V}(\text{Sco X-1}) + (B-V)_{1636-53} - (B-V)_{\text{Sco X-1}} .$$

With E_{B-V}(Sco X-1) = 0.35 (Willis *et al.* 1980) we obtain for 4U/MXB 1636−53: $E_{B-V} = 0.8$, corresponding to $K_e \approx 19$.

Thus the estimate of the interstellar extinction factor ranges between ~4 and ~19. In our modeling of the optical/X-ray burst, we have adopted an extinction factor $K_e = 13$ (see eq. [11]). The effect of smaller or larger values is discussed in § VI.

d) Observed Optical and X-Ray Fluxes—Model Parameters

The determination of a model which relates the measured narrowband optical flux F_o to the broad-band X-ray flux falls into the domain of nonlinear digital signal processing. One must be careful in accounting for the effects of Poisson noise on the errors in the values of the model parameters. The equations which relate F_o and F_x and thereby model the reprocessing object are derived from equations (4) and (5) of § III.

$$T_e(t) = \left[\frac{G(t)}{G_{\max}} + \left(\frac{T_q}{T_{\max}}\right)^4\right]^{1/4} \times T_{\max} , \quad (8a)$$

where

$$G(t) = \int_{-\infty}^{\infty} \hat{F}_x(u) g(t-u) du \equiv \frac{1}{s} \int_{-s/2}^{s/2} \hat{F}_x(u + t - \Delta) du \,, \tag{8b}$$

$$g(t) = \begin{cases} \frac{1}{s} & \text{for } \left(\Delta - \frac{s}{2}\right) < t < \left(\Delta + \frac{s}{2}\right), \\ 0 & \text{otherwise} \end{cases} \tag{8c}$$

and

$$G_{\max} = \left[1 - \left(\frac{T_q}{T_{\max}}\right)^4\right]^{-1} \times \text{maximum value of } G(t) \tag{8d}$$

Assuming that the optical flux in the absence of X-ray heating and the reprocessed flux are emitted by the same object, the parameter H in equation (4b) is eliminated in equation (8a) in favor of parameter T_q. Therefore equations (4) and (5) combined are equivalent to equations (8a)–(8d). $G(t)$ operates on the bolometric X-ray flux (assuming isotropic emission) and introduces a delay (Δ) and a rectangular smearing (full width s). $\hat{F}_x$ is a model of the X-ray flux as a function of time. The model of the optical flux is

$$\hat{F}_o = Q B_\nu(T_e) \Delta\nu \quad \text{where} \quad Q = \frac{A_{\text{eff}}}{d^2} \,. \tag{9}$$

The parameters T_q, $T_{\max}$, s, Δ, and Q are varied as well as the model of the X-ray flux $\hat{F}_x(t)$ until χ^2 is minimized. χ^2 is a sum over all optical and X-ray measurements with the variances determined by the expected Poisson fluctuations.

$$\chi^2 = \sum \left(\frac{F_x - \hat{F}_x}{\sigma_x}\right)^2 + \sum \left(\frac{F_o - \hat{F}_o}{\sigma_o}\right)^2 . \tag{10}$$

The variances σ_x and σ_o are determined from the counting statistics of F_x and F_o respectively. The present method is particularly useful since the determination of the five parameters is independent of the distance to the source, its surface geometry, or the interstellar extinction.

V. RESULTS

An intrinsic property of the present method is the irregular fluctuation of χ^2 as a function of delay Δ for values of smearing s near zero. If the signal-to-noise ratio is marginal, the determination of the lower bound for the smearing parameter s is hampered by the presence of these fluctuations in χ^2. As the signal-to-noise ratio increases, the domain of instability eventually moves outside the 90% confidence region, thereby stabilizing the procedure. The character of these expected fluctuations has been determined by ideal simulations including Poisson counting noise. We have also investigated the method of constraining the smoothness of the model parameters $\hat{F}_x$, e.g., by adequately filtering the Poisson noise. This removes the fluctuations for smearing values s near zero and gives approximate confidence regions for all parameters. This, however, may introduce a small bias in s depending on the filter used and hence limits the capability of determination of s near zero. However, for the signal-to-noise ratio of the present data, this method does not affect the best fit values of T_q, $T_{\max}$, Δ, and Q significantly. Due to these complications and the possibility of systematic effects, we conclude that the data presented in this paper are of insufficient quality to reject the possibility of smearing s equal to zero, although this is very unlikely.

In view of this difficulty in determining s as well as strong interrelations between s and other parameters $T_{\max}$, Q, and T_q, the burst data near 1979 June 28, UT 0155 were analyzed for different values of s separately. For s near zero, the upper limit of $T_{\max}$ is undetermined. As s increases, finite confidence regions for all the model parameters can be obtained. The best fit value and the error for the optical delay Δ are determined almost independently of values of s, and the result implies that the separation between the X-ray and the optical emission regions is larger than about 1 lt-sec. This enables us to estimate the upper limit for $T_{\max}$ in terms of equation (2). The χ^2 fitting shows that the ratio of $T_{\max}$ to T_q is always larger than 2.2 for any value of s less than 4 s. Therefore, the optical luminosity in the absence of X-ray heating is less than 4% of the X-ray induced optical luminosity at burst maximum. Since the term σT_q^4 in equation (2) is negligible, an upper limit for T_e of 1.8×10^5 K is obtained for the smallest allowed value for r (=0.75 lt-sec) for an assumed distance to the source of 10 kpc and $f \cos\gamma$ equal to unity. Allowing for a realistic upper limit for $T_{\max}$, finite 90% confidence domains are defined for all the model parameters except for T_q even for the case of s equal to zero as listed in Table 4.

In Figures 3 and 4 we show an example of the result of the χ^2 fitting. The optical flux F_o and the bolometric

TABLE 4

BURST ON 1979 JUNE 28, 0155 UT

Model Parameter	Symbol	Value
Maximum optical temperature	$T_{\max}$	$(7.4^{+4.3,-1.7}) \times 10^4$ K
Optical delay	Δ	(2.4 ± 0.6) s
Rectangular smearing width	s	$\lesssim 4$ s
Normalization constant	Q	$(6.6^{+4.2,-3.2}) \times 10^{-24}$
Quiescent temperature (no X-ray heating)	T_q	$< T_{\max}/2.2$

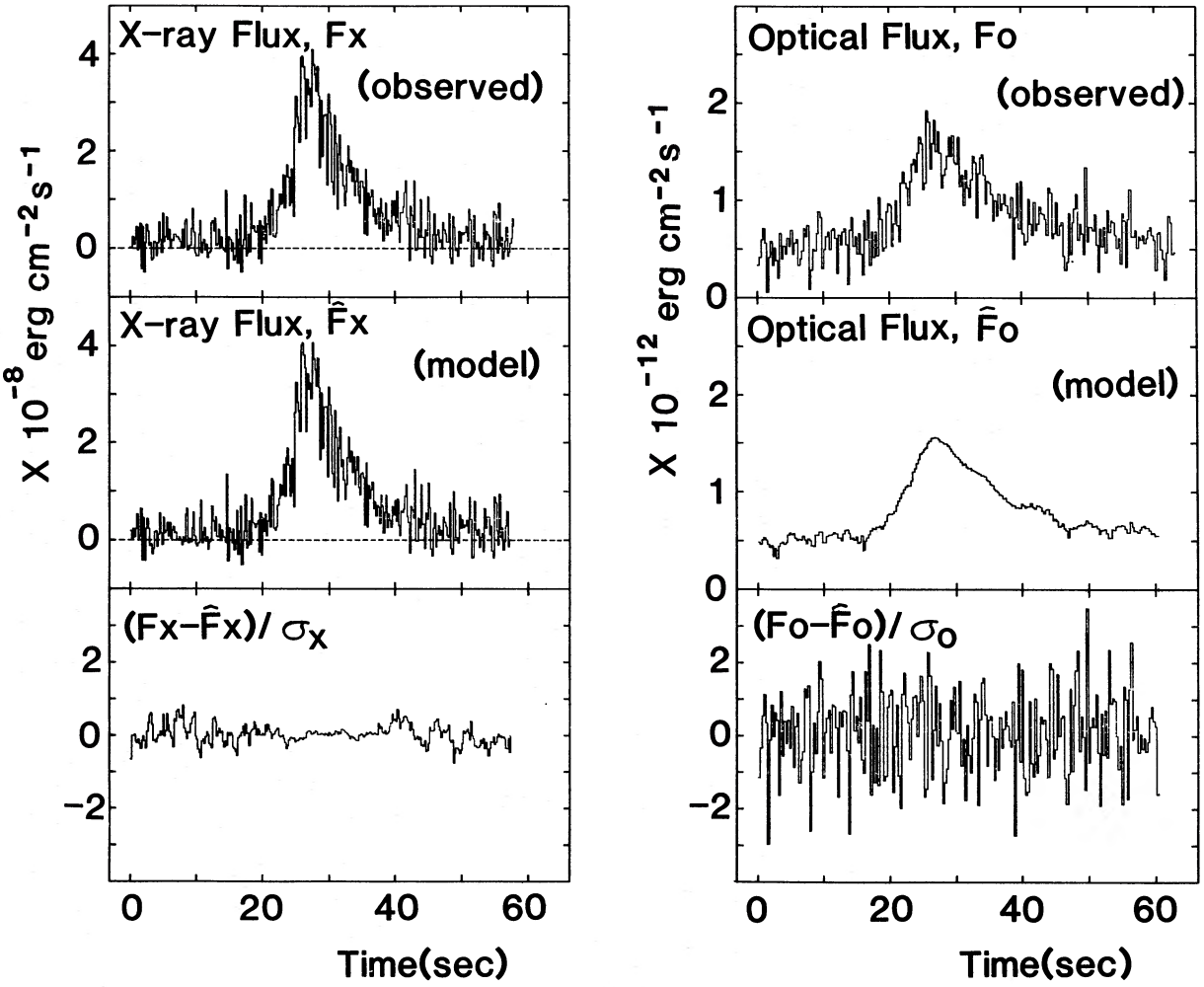

FIG. 3.—Comparison of observed and model fluxes for simultaneous X-ray/optical burst of 1979 June 28 (see Fig. 1). The observed X-ray flux, F_x, is calculated according to eq. (6) and approximates the total integrated flux assuming a blackbody spectrum. The optical flux, F_0, is calculated according to eq. (7) (the vertical scale is divided by 13); it approximates the integrated flux in a narrow optical passband (see Table 3). The model optical flux, F_0, is calculated according to eq. (9) (scale divided by 13); it depends on the value of the X-ray model and the free parameters listed in Table 4. For the sake of drawing a representative figure, the model is displayed for the values of the parameters which minimize the total χ^2 function, fixing parameters of smearing width $s = 3$ s and optical delay $\Delta = 3$ s (reduced χ^2 value 1.3 with 225 degrees of freedom corresponding to 563 measurements minus 338 parameters). The deviations (not squared) of each X-ray and optical term of χ^2 are displayed.

X-ray flux F_x (see § IV) are displayed in the upper panels of Figure 3. The middle panels of Figure 3 are the best fit models for the X-ray ($\hat{F}_x$) and the optical ($\hat{F}_o$) data for $T_q = 0$ and $s = 3$ s. The bottom panels indicate the goodness of fit in units of the standard deviation of each measurement (expected from the approximate Gaussian nature of the Poisson fluctuations). The model fits both the X-ray and optical signals well before, during, and after the burst. The reduced χ^2 value is 1.3 with 225 degrees of freedom (563 measurements minus 338 parameters). This value is formally in excess of unity by a considerable amount. However, a modest 10% increase in the measurement errors in excess of the expected Poisson component would explain the discrepancy.

A single model parameter for each bin of X-ray data (333 points) $\hat{F}_x(t)$ represents the total bolometric X-ray flux. The fourth root of $F_x(t)$ is proportional to the X-ray temperature if the spectrum is approximately that of a blackbody. The profile of the X-ray temperature as a function of time is displayed in Figure 4. The profile is normalized to a peak temperature of $\sim 3 \times 10^7$ K ($kT \sim 2.7$ keV) determined from the ratio of the count rates in the two X-ray energy bands. The rapid fluctuations in the model X-ray temperature during the pre- and postburst periods are due to the poor statistical determination of the flux of the persistent X-ray source during each short integration period (Δ_x). The time averaged X-ray temperature before and after the burst is well determined. The reprocessing temperature,

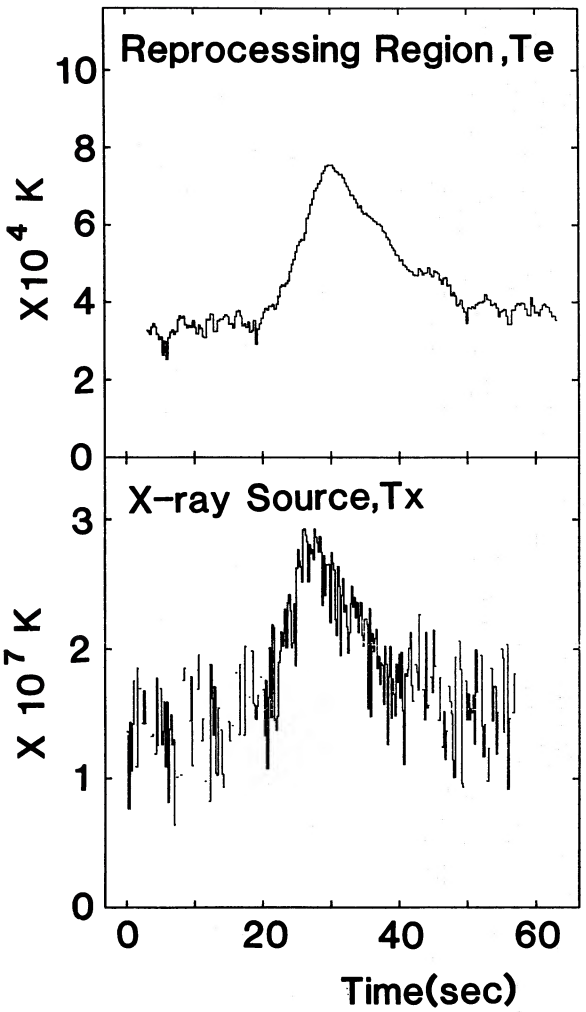

FIG. 4.—*Blackbody temperature.* The temperature, T_e, of the reprocessing region and the temperature, T_x, of the X-ray source as functions of time. The temporal profile of T_e is determined from the value of T_{max} and eq. (8). Formally, the absolute scale at T_e is determined from the model as a consequence of the relative response of the optical signal to the X-ray signal and therefore does not depend on distance to the source or the amount of optical extinction. The relative X-ray temperature is determined as the fourth root of the model of the X-ray flux $\hat{F}_x$. The profile is approximately normalized by fitting the two broad-band X-ray channels to a blackbody spectrum. The relative excursion of the T_x and T_e is approximately the same as expected. The profile of T_e is delayed and smeared relative to that of T_x. As in Fig. 3, s and Δ were fixed at 3 s for the sake of drawing a representative figure.

T_e, is also displayed in Figure 4 based on the equations in § IV. In this example s is fixed at 3 s. This definite value of s solves the strong interrelation between s and T_{max}, and the determination of T_{max} depends only on the relative temporal profiles of the optical and X-ray signals. The reprocessing region jumps from a temperature of $\sim 30 \times 10^3$ K in the presence of the persistent X-ray flux to a peak temperature of $\sim 75 \times 10^3$ K during the burst. The optical signal is delayed relative to the X-ray by $\Delta \sim 2.4$ s. This method determines the temporal profile of the temperature independent of the distance to the source, its surface geometry, or the interstellar extinction.

The effective area, $A_{\rm eff}$, can be calculated if we know the extinction (K_e) and the distance to the source (d) (see § IV).

$$A_{\rm eff} = d^2 Q \approx 6 \times 10^{21} \left(\frac{K_e}{13}\right) \left(\frac{d}{10\ \rm kpc}\right)^2 \ \rm cm^2 \ . \quad (11)$$

Here d is in kpc. The actual area of the reprocessing object must be somewhat larger than the effective area (see eq. [4a]).

VI. DISCUSSION

The correlated optical and X-ray bursts are useful as diagnostic tools to probe the structure of the surroundings of the X-ray burst source. Within the framework of the low-mass binary system obvious sites for the reprocessing of X-rays are the companion star and the accretion disk around the neutron star.

We have performed numerical calculations of the response function of reprocessing bodies, taking into account geometric delay and ignoring the contributions of both radiative delay and radiative smearing. We believe that these assumptions are justified (see § III*a*). However, we like to point out that it can not be excluded that the observed delay between the optical and X-ray signals is largely due to radiative smearing, though we believe that is unlikely; but until thorough calculations are made, one can not be certain.

Ordering the contributions of all surface elements according to their geometric delays produces a distribution function of the optical emission which is the response of the reprocessing body to a δ-function input of X-rays.

Since the observed delays of the optical bursts are always of the order of a few seconds, the reprocessing must take place within a few light-seconds of the X-ray source. Much evidence has become available during the last few years that X-ray burst sources (more generally galactic bulge sources) are low-mass close-binary systems in which mass is transferred from a Roche-lobe filling, probably main-sequence, companion star onto the compact X-ray emitting object (for recent reviews, see Lewin and Joss 1981, 1982). Within the framework of this model, obvious candidates for the reprocessing site are the surface of the companion star and the accretion disk surrounding the burst source.

Based on the above mentioned numerical calculation three main differences in the properties of optical bursts are expected. The first is that in the case of reprocessing in the companion star, the ratio of optical to X-ray flux is expected to be always less than $\sim 10^{-3}$, whereas in the case of a disk much higher values are possible (depending on the thickness of the disk).

Second, the smearing of optical burst signals originating from companion stars is expected to be small. From the numerical calculations of the optical response to a δ-function X-ray burst, we find that in that case, the

ratio of smearing to delay is always less than ~ 0.25. In the case of an accretion disk, however, this ratio is expected to be $\gtrsim 1$, depending mainly on the inclination of the system. Recently, Pedersen, van Paradijs, and Lewin (1981) have reported a possible ~ 4 hour periodic (orbital?) modulation in the optical flux from 4U/MXB 1636−53. They suggest that this may be the result of an accretion disk which is not axisymmetric and is perhaps thicker where matter is injected into the disk (similar to an earlier suggestion made for 4U 1822−37 by White *et al.* 1981). If this is so, different values for the delay Δ would be expected for various orbital phases. To within the accuracy of their determination, the delays observed for the three analyzed bursts are nearly equal: 3 ± 1.5 s for the burst on 1979 June 21 near UT 0148; 4 ± 1.5 s for the burst on 1979 June 21 near UT 0334; and 2.4 ± 0.6 s for the burst on 1979 June 28 near UT 0155. These measurements of Δ are of insufficient quantity and quality to evaluate possible orbital effects.

In the following we will show how our conclusions, together with the observed optical burst parameters, can be used to constrain parameters of the binary system.

a) Mass of the Companion Star

If the accretion disk is the site of the X-ray reprocessing, the average delay of the optical signal depends on the orbital inclination and on the radial distribution of matter in the disk. The largest values of the delay are expected if the reprocessing takes place mostly near the outer parts of the disk and if the part closest to the Earth is almost invisible because of self-occultation (large inclination). This shows that half the delay provides a lower limit (in light-seconds) to the radius of the accretion disk.

The latter result is of interest since for a variety of reasons (see, e.g., Paczynski 1977; Gehrend and Boynton 1976; Crosa and Boynton 1980; Lin and Pringle 1976) it appears that accretion disks almost (perhaps even completely) fill their Roche lobe. It seems safe to conclude that the ratio of the radius of the accretion disk to that of the Roche lobe is in the range of 0.5 to 1.0. Thus, constraints on the size of the accretion disk also constrain the effective radius of the Roche lobe, R_x, around the X-ray source.

For given values of R_x and masses M_x of the X-ray source and M_c of the companion star, the effective radius of the companion's Roche lobe, R_c, is a function of the mass ratio $q = M_c/M_x$ only. From Paczynski's (1971) relations, we find the following relation between R_c and R_x:

$$\frac{R_c}{R_x} = \begin{cases} 0.462\left(\dfrac{q}{1+q}\right)^{1/3}(0.38\text{–}0.2\log q)^{-1} & q \le 0.5 \\ (0.38 + 0.2\log q)(0.38\text{–}0.2\log q)^{-1} & 0.5 < q < 3 \\ 2.16(1+q)^{1/3}(0.38 + 0.2\log q) & 3 < q < 20\,. \end{cases} \quad (12)$$

We take a fixed value 1.4 $M_\odot$ for M_x (this seems reasonable in view of the relatively small spread in the observed values of neutron star masses; see Joss and Rappaport 1979). If we also assume that the companion star fills its Roche lobe, a measurement of (or a constraint on) the value of R_x provides (or constrains) a relationship between the mass, M_c, and the radius of the companion star, R_c.

In Figure 5 we have drawn mass-radius relations for zero-age main sequence stars (ZAMS) with masses between 4 $M_\odot$ and 10 $M_\odot$ (Whyte and Eggleton 1980), for low-mass companions ($\le 0.4\ M_\odot$) which evolve into even lower mass stars by accretion which is driven by gravitational radiation (Rappaport, Joss, and Webbink 1982), and for white dwarfs assuming 70% fraction of hydrogen (see Rappaport, Joss, and Webbink 1982). For stars later than M0, the model calculations of Rappaport, Joss, and Webbink differ from main-sequence equilibrium solutions in that the star is slightly larger than a ZAMS star of the same mass. If some other mechanism of rapid angular momentum loss besides gravitation radiation is possible, then evolutionary tracks would probably deviate to even larger radii. Similarly, any nuclear evolution of the system also tends to increase the radius for a given mass star.

The dashed line indicates the M_c, R_c relation for a Roche lobe radius of the X-ray source (R_x) of ~ 1 lt-sec. For larger and smaller values of R_x, the dashed line can be moved approximately parallel to itself. The R_x axis indicated in the figure can be used to choose the desired value of R_x. The dotted line indicates the M_c, R_c relation for a binary period of ~ 1 hour (assuming Roche geometry). For other binary periods the "Binary Period" axis, as indicated, can be used (the dotted line can be moved parallel to itself). Our data indicate that the delay Δ is about 2.4 s. Depending on the orientation of the orbit (inclination), the radius of the disk could therefore be somewhere between 1.2 and 2.4 s. If this radius is ~ 0.5 to 1.0 times that of the Roche lobe of the X-ray star, then this Roche lobe radius should be no smaller than ~ 0.6 s. This would allow the companion star (if it is on the main sequence) to be any late main-sequence star. The mass of the companion could be as low as $\sim 0.1\ M_\odot$ if its evolution is modified by accretion.

Based on the lack of stellar absorption features in the spectrum of 4U/MXB 1636−53, Canizares, McClintock, and Grindlay (1980) have concluded that the companion star of 4U/MXB 1636−53 is of spectral type later than F0. Therefore, we conclude that the companion has a mass between ~ 0.1 and 2 $M_\odot$ and is in a binary with a period between ~ 1 hour and 10 hour (see Rappaport, Joss, and Webbink 1981 for a detailed discussion of the existence of a minimum binary period). As already mentioned above, recently, Pedersen, van Paradijs, and Lewin (1981) have detected a strong modulation in the optical flux which appears to be periodic (period ~ 3.8 hours). If (1) this is the orbital period of the system, (2) the companion star fills its Roche lobe, and (3) the companion is a main-sequence star, then the companion of 4U/MXB 1636−53 has a mass of $\sim 0.4\ M_\odot$ (corresponding to an M0 V star). This is independent of any assumption regarding the mass of the neutron

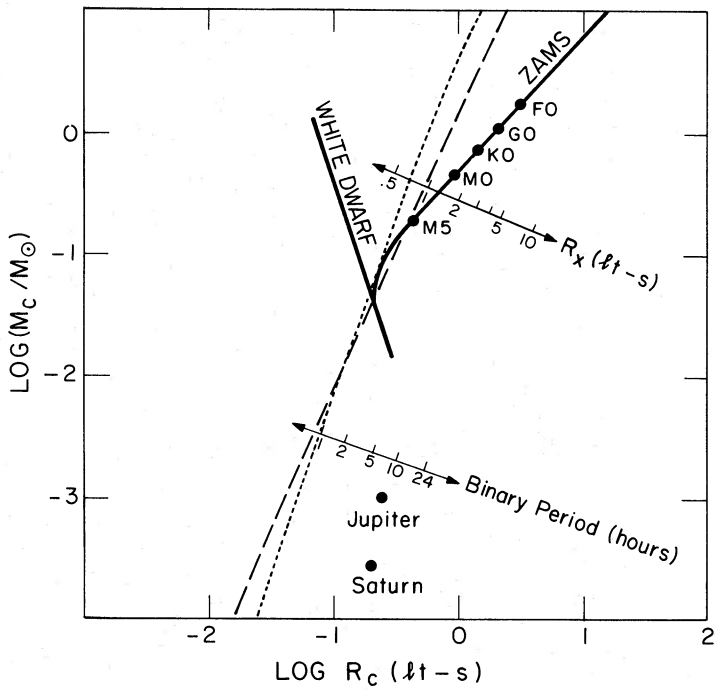

FIG. 5.—Allowed values of a companion mass, M_c, and radius, R_c, assuming that the companion of an $\sim 1.4\ M_\odot$ neutron star has filled its Roche lobe. The binary period of the system and the radius of the Roche lobe, R_x, of the compact X-ray source are indicated. Note that the companion radius, R_c, is indicated in lt-s to facilitate a comparison with the delay Δ. The dashed line indicates the M_c, R_c relation for a Roche lobe radius of the X-ray source (R_x) of ~ 1 lt-s. For larger and smaller values of R_x the dashed line can be moved approximately parallel to itself. The R_x axis indicated can be used to choose the desired value of R_x. The dotted line indicates the M_c, R_c relation for a binary period of ~ 1 hour (assuming Roche geometry). The dotted line can be moved parallel to itself (use "Binary Period" axis). The curved portion of the solid line which connects M5 to the white dwarf branch is from Rappaport, Joss, and Webbink (1982).

star. This result is in agreement with our estimate of the mass of the companion. This result is also consistent with the available information on companion stars of the bursting soft X-ray transients Aql X-1 and Cen X-4 (Thorstensen *et al.* 1978; van Paradijs *et al.* 1980). The spectral types of these companions (G7–K3 V and K3–K7 V, respectively) indicate masses between ~ 0.5 and $\sim 1\ M_\odot$. A low-mass companion star is also found in the nonbursting transient X-ray source A060−00 (Oke 1977) which seems to be a member of the class of galactic bulge sources of which the burst sources are a subset (see Lewin and Joss 1981, 1982). (It should be kept in mind that if these companion stars have already evolved their masses could be substantially less.)

b) *Effective Area of the Reprocessing Region and the Thickness of the Accretion Disk*

Using the values for extinction as derived above, and assuming a distance to the source of 10 kpc, we find for the effective area $A_{\rm eff}$ (see eq. [11]) as observed at burst maximum, values ranging from $\sim 2 \times 10^{21}$ cm^2 to $\sim 9 \times 10^{21}$ cm^2, corresponding to projected circular areas with radii between ~ 0.8 lt-sec and ~ 1.8 lt-sec. This result is consistent with the size estimate of the accretion disk based on the observed value for the delay in the optical signal.

The optical luminosity from such a disk would be $L(t) = (A_{\rm eff}/\cos\ i)\sigma T_{\rm eff}^4$, where cos i is the projection factor due to foreshortening of the disk. The luminosity of the X-ray source, L_x, equals $4\pi d^2 F_x(t)$, where d is the distance to the source (for which we have taken 5 kpc) and $F_x(t)$ the observed X-ray flux (interstellar absorption is negligible). If we assume that a fraction f of the X-ray flux incident on the disk is absorbed and reprocessed, we can calculate the solid angle Ω of the disk as seen from the X-ray star.

$$\frac{2Q\sigma T^4}{4\pi F_x \cos i} = \frac{f\Omega}{4\pi} . \tag{13}$$

With the measured value of Q and the ratio T^4/F_x, we find that the product f cos $i(\Omega/4\pi)$ equals $\sim 5.2 \times 10^{-2}$, corresponding to an angular thickness of the disk from the central plane as seen from the neutron star of $\theta = (3^{+5,\,-1.5})/f$ cos $i°$. It is very likely that the value of f cos i is less than 0.5 (Milgrom and Salpeter 1975; London, McCray, and Auer 1980). Thus θ is between $\sim 3°$ and $\sim 16°$. Milgrom (1978) suggested that in this class of sources the low-mass companion stars lie in the X-ray shadow of the accretion disk. This could explain why X-ray eclipses are in general not observed from these systems (for recent reviews see Lewin and Joss 1981, 1982). The values for θ that would meet Milgrom's criterion would be of order of 10°. This is in agreement with our results.

H. P. wishes to thank the Danish "Forskningssekretariatet" for use of the telescope during its initial test period and ESO's technical groups at La Silla for extensive support. L. Cominsky acknowledges support from Zonta International during much of this work. We are grateful to Richard London who pointed out some difficulties in evaluating the radiative reprocessing time; his valuable comments have been incorporated. We wish to thank B. Parsons, M. Carracino, and S. Black for assistance in preparation of the manuscript and Zahir Ebrahim for help in preparing the figures. This work was supported in part by grants from the National Aeronautics and Space Administration under contract NAS5-24441 and from the Japan-U.S. Cooperative Science Program under NSF grant INT 8017890/R-EPA-0200.

APPENDIX

Upon entering the absorber, a photon may scatter many times. Its chance to be absorbed at each interaction is $\kappa/(\kappa+\sigma)$. Here κ is the absorption opacity and σ the scattering opacity of the photon. After $N_1 = 1 + (\sigma/\kappa)$ scatterings (on the average), the photon will have been absorbed, having traveled through a random-walk path down to optical depth $\tau\sqrt{N_1}$ (Mihalas 1978).

We have calculated a representative value of N_1 corresponding to a depth where most of the X-ray energy is absorbed by

$$\bar{N}_1 = 1 + \frac{\int_0^\infty [\sigma/\kappa(E)]F(E)dE}{\int_0^\infty F(E)dE} . \tag{A1}$$

Here $F(E)$ is the incident X-ray flux, for which we have taken blackbody spectra with values for kT of 1, 2, and 3 keV, which cover the range of interest of X-ray bursts.

If we take a solar composition (Withbroe 1971) for the absorber, the absorption cross section over the whole X-ray energy interval of interest (1–20 keV) is of the same order of magnitude as, or larger than, the Thomson cross section for electron scattering.

Using the results on $\kappa(E)$ by Fireman (1974) we find that $\bar{N}_1 \sim 1$ for a blackbody temperature of $kT = 1$ keV and ~ 2 for $kT = 3$ keV. This rather crude result is supported by detailed self-consistent numerical calculations of X-ray illuminated stellar atmospheres (London, McCray, and Auer 1980), which show that almost all X-ray energy is absorbed at a column density of ~ 2.5 g cm^{-2}, corresponding to an optical depth for electron scattering $\tau_{es} \sim 1.0$. Since the X-ray spectrum used in these calculations is "harder" than that observed in X-ray bursts, this value for the optical depth at which the X-ray energy is deposited should be higher than the values relevant here. Thus, if the gas is of normal composition, the X-ray burst energy will be deposited after the X-rays have traversed a total pathlength corresponding to $\tau_{es} \lesssim 1$. Allowing for an oblique angle θ of incidence ($\cos\theta = \mu$), the corresponding optical depth of energy deposition is $\tau_{es} \lesssim \mu$.

If the reprocessing occurs in the surface layers of a companion star or an accretion disk, it seems justified to approximate the absorbing layer as a homogeneous slab of density ρ. The geometric depth of energy deposition is given by $\sigma\rho\Delta x \leq \mu$, i.e., $\Delta x < 2.5\mu/\rho$ (in cgs units). We have substituted $\sigma = 0.4$ cm^2 g^{-1}. The corresponding time Δt for X-ray absorption is given by $\Delta t \leq 2.5\mu/\rho c$. For the density we take the value at $\tau_{es} = \mu$ in the isothermal atmosphere with the same temperature T and with gravity acceleration g: $\rho = 1.5 \times 10^{-8}(g\mu/T)$. Thus the X-rays will be absorbed after a time:

$$\Delta t_{abs} = \frac{2.5}{1.5 \times 10^{-8}\ \mathrm{cg}/T} \simeq 6 \times 10^{-3}\ \mathrm{g}^{-1} \times T\ \mathrm{s} \tag{A2}$$

For a stellar companion (for which the mass is low, $M \lesssim 1\ M_\odot$) we have $g \sim 10^{4.5}$. The temperatures of such companions are unlikely to be more than 50,000 K, and the values for Δt_{abs} are negligible in this case. In the case of an accretion disk the effective gravity is given by the component perpendicular to the orbital plane of the gravity acceleration to the central object. For typical values of M and R ($1\ M_\odot$ and $1\ R_\odot$) we expect $g \sim 10^3$ even for very thin disks ($\sim 1°$ opening angle), and $\Delta t_{abs} \lesssim 0.2$ s at temperatures of the absorbing disk as high as 5×10^4 K.

In order to make an estimate of the time it takes for the absorbed X-rays to emerge as optical photons, we have made the diffusion approximation. The mean free path of an average photon is given by $\Delta l = 1/\bar{\kappa}\rho$, where $\bar{\kappa}$ is the Rosseland mean opacity. In order to reach the surface from an optical depth $\tau_{es} = \mu$ (corresponding to geometric depth $\Delta x = \mu/\sigma\rho$), the average photon has to traverse a total number, $N\ [=(\mu\bar{\kappa}/\sigma)^2]$, of mean free path lengths. The time for the average optical photon to emerge at the surface can be estimated by

$$c\Delta t_{esc} = N\frac{1}{\bar{\kappa}\rho} = 6.25\frac{\bar{\kappa}\mu^2}{\rho}\ (\mathrm{cgs\ units}) . \tag{A3}$$

With our above estimate for ρ we find

$$\Delta t_{\rm esc} = \frac{6.25\bar{\kappa}\mu}{1.5 \times 10^{-8}\ {\rm gc}/T}\ ({\rm cgs\ units})\ . \tag{A4}$$

Using the Rosseland opacity tables of Cox and Stewart (1970) we find that over a temperature range from $T = 10^4$ to 5×10^4 K and for log $g = 3$ to 4.5, $\Delta t_{\rm esc}$ is always less than 0.6 s.

REFERENCES

Allen, C. W. 1973, *Astrophysical Quantities* (London: Athlone).
Canizares, C. R., McClintock, J. E., and Backman, D. E. 1978, *Ap. J. (Letters)*, **223**, L75.
Canizares, C. R., McClintock, J. E., and Grindlay, J. E. 1980, *Ap. J.*, **234**, 546.
Chandrasekhar, S. 1943, *Rev. Mod. Phys.*, **15**, 1.
Chester, T. J. 1978, *Ap. J.*, **222**, 652.
———. 1979, *Ap. J.*, **227**, 569.
Crosa, L., and Boynton, P. E. 1980, *Ap. J.*, **235**, 999.
Cox, A. N., and Stewart, J. N. 1970, *Ap. J. Suppl.*, **19**, 243.
Fireman, E. L. 1974, *Ap. J.*, **187**, 57.
Gehrend, D., and Boynton, P. E. 1976, *Ap. J.*, **209**, 562.
Hackwell, J. A., Grasdalen, G. L., Gehrz, R. D., van Paradijs, J., Cominsky, L., and Lewin, W. H. G. 1979, *Ap. J. (Letters)*, **233**, L115.
Hammerschlag-Hensberge, G., McClintock, J. E., and van Paradijs, J. 1982, *Ap. J. (Letters)*, **254**, L1.
Hoffman, J. A., Lewin, W. H. G., and Doty, J. 1977*a*, *Ap. J. (Letters)*, **217**, L23.
———. 1977*b*, *M.N.R.A.S.*, **179**, 57P.
Hoffman, J. A., Marshall, H., and Lewin, W. H. G. 1978, *Nature*, **271**, 630.
Joss, P. C., and Rappaport, S. A. 1979, *Astr. Ap.*, **71**, 217.
Kondo, I., *et al.* 1981, *Space Sci. Instr.*, **5**, 211.
Lewin, W. H. G. 1979, *IAU Circ.* 3334.
Lewin, W. H. G., and Clark, G. W. 1980, *Proc. 9th Texas Symp., Munich* (*Ann. NY Acad. Sci.*, **336**, 451).
Lewin, W. H. G., and Joss, P. C. 1981, *Space Sci. Rev.*, **28**, 3.
———. 1982, in *Accretion Driven Stellar X-Ray Sources*, ed. W. H. G. Lewin and E. P. J. van den Heuvel (Cambridge: Cambridge University Press), in press.
Lin, D. N. C., and Pringle, J. E. 1976, in *IAU Symposium 73, Structure and Evolution of Close Binary Systems*, ed. P. Eggleton, S. Mitton, and J. Whelan (Dordrecht: Reidel), p. 237.
London, R., McCray, R., and Auer, L. 1981, *Ap. J.*, **243**, 970.
Lucke, P. B. 1978, *Astr. Ap.*, **64**, 367.
McClintock, J. E., Canizares, C. R., Bradt, H. V., Doxsey, R. E., Jernigan, J. G., and Hiltner, W. A. 1977, *Nature*, **270**, 320.
McClintock, J. E., Canizares, C. R., Li, F. K., and Grindlay, J. E. 1980, *Ap. J. (Letters)*, **235**, L81.
McClintock, J. E., Grindlay, J. E., Canizares, C. R., van Paradijs, J., Cominsky, L., Li, F. K., and Lewin, W. H. G. 1979, *Nature*, **279**, 47.
Middleditch, J., Mason, K. O., Nelson, J., and White, N. 1981, *Ap. J.*, **244**, 1001.
Mihalas, D. 1978, *Stellar Atmospheres* (2d ed.; San Francisco: Freeman).
Milgrom, M. 1978, *Astr. Ap.*, **67**, L25.
Milgrom, M., and Salpeter, E. E. 1975, *Ap. J.*, **196**, 583.
Neckel, Th., and Klare, G., 1980, *Astr. Ap. Suppl.*, **42**, 251.
Oke, J. B. 1974, *Ap. J. Suppl.*, **27**, 31.
———. 1977, *Ap. J.*, **217**, 181.
Paczynski, B. 1971, *Ann. Rev. Astr. Ap.*, **9**, 183.
———. 1977, *Ap. J.*, **216**, 822.
Pedersen, H., the Hakucho Team, Cominsky, L., Doty, J., Jernigan, G., van Paradijs, J., and Lewin, W. H. G. 1979, *IAU Circ.* 3399.
Pedersen, H., van Paradijs, J., and Lewin, W. H. G. 1981, *Nature*, **294**, 725; see also *IAU Circ.* 3628.
Pedersen, H., van Paradijs, J., Motch, C., Cominsky, L., Lawrence, A., Lewin, W. H. G., Oda, M., and the Hakucho Team. 1982, *Ap. J.*, **263**, 340.
Rappaport, S. A., Joss, P. C., and Webbink, R. 1982, *Ap. J.*, **254**, 616.
Stone, R. P. S. 1977, *Ap. J.*, **218**, 76.
Swank, J. H., Becker, R. H., Boldt, E. A., Holt, S. S., Pravdo, S. H., and Serlemitsos, P. J. 1977, *Ap. J.*, **212**, L73.
Sunyaev, R. A., and Titarchuk, L. G. 1980, preprint.
Thorstensen, J., Charles, P., and Bowyer, S. 1978, *Ap. J. (Letters)*, **220**, L131.
———. 1980, *Ap. J.*, **238**, 964.
van Paradijs, J. 1978, *Nature*, **274**, 650.
———. 1981, *Astr. Ap.*, **103**, 140.
van Paradijs, J., Verbunt, F., van der Linden, T., Pedersen, H., and Wamsteker, W. 1980, *Ap. J. (Letters)*, **241**, L161.
White, N. E., Becker, R. H., Boldt, E. A., Holt, S. S., Serlemitsos, P. J., and Swank, J. 1981, *Ap. J.*, **247**, 994.
Whyte, G. A., and Eggleton, P. P. 1980, *M.N.R.A.S.*, **190**, 801.
Wickramasinghe, D. T., and Whelan, J. 1975, *M.N.R.A.S.*, **172**, 175.
Withbroe, G. L. 1971, in *The Menzel Symposium*, ed. K. B. Gebbie, NASA SP-353 (Washington: U.S. Government Printing Office), p. 127.
Zuiderwijk, E. J., Hammerschlag-Hensberge, G., van Paradijs, J., Sterken, C., and Hensberge, H. 1977, *Astr. Ap.*, **54**, 167.

A. Beardsley, L. Cominsky, J. Doty, J. G. Jernigan, W. H. G. Lewin, and J. van Paradijs: Department of Physics and Center for Space Research, Massachusetts Institute of Technology, Cambridge, MA 02139

S. Hayakawa, H. Kunieda, F. Makino, K. Masai, F. Nagase, and Y. Tawara: Department of Astrophysics, Faculty of Science, Nagoya University, Chikusa, Nagoya 464, Japan

H. Inoue, K. Koyama, K. Makishima, M. Matsuoka, K. Mitsuda, T. Murakami, M. Oda, Y. Ogawara, T. Ohashi, N. Shibazaki, and Y. Tanaka: Institute for Space and Astronautical Science, Komaba, Meguro-Ku, Tokyo 153, Japan

I. Kondo: Institute for Cosmic Ray Research, University of Tokyo, Tanashi, Tokyo 188, Japan

J. Lub and H. Pedersen: European Southern Observatory, Casilla 16317, Santiago, Chile

S. Miyamoto, H. Tsunemi, and K. Yamashita: Department of Physics, Faculty of Science, Osaka University, Toyonaka, Osaka 560, Japan